

## SIGNATURES OF SMOLDERING/PYROLYZING FIRES FOR MULTI-ELEMENT DETECTOR EVALUATION\*

Thomas Cleary, William Grosshandler, Marc Nyden, and William Rinkinen, Building & Fire Research Laboratory, National Institute of Standards and Technology, USA.

### ABSTRACT

Levels of CO, CO<sub>2</sub>, H<sub>2</sub>O, hydrocarbons, smoke, temperature and velocity produced in the plumes of smoldering/pyrolyzing wood and smoldering cotton fires are reported, following test protocols described for evaluating automatic fire detection systems. The repeatability of the wood fires is high, but the smoldering cotton results can vary considerably depending upon the exact configuration of the fuel. The water vapor builds up most quickly in both fires, with CO and CO<sub>2</sub> growing more slowly in volume fraction but at a close to constant ratio. Temperatures increase steadily on the plume centerline, and the vertical velocities correlate roughly with the square root of the difference in plume and surrounding temperatures. The data are compared to previous results, and a method for using these measurements to evaluate multi-criteria fire detection systems is proposed.

### BACKGROUND

Most common fire detectors employ single elements to sense changes in temperature or particulate levels at a point within a room. Standardized tests such as Underwriters Laboratory (UL) 217<sup>1</sup> and Comité Européen de Normalization (CEN) 54<sup>2</sup> were developed to certify the operation of the different designs supplied by various equipment manufacturers. New detector designs are now beginning to come on the market that utilize more than one sensing element; e.g., an ionization chamber and a temperature sensor, an ionization and light scattering device, or a CO plus a smoke sensor. By properly processing two independent signals indicative of a fire, the status (i.e., fire or no-fire) can be predicted with a much higher degree of certainty. Standard test methods have not yet been adopted for quantifying the performance of multi-element fire detectors.

A workshop<sup>3</sup> was held at NIST early in 1995 to identify the needs of users and specifiers of fire detection systems, and to develop a research agenda to overcome existing technological barriers to meet those needs. Test methods for multi-criteria detectors and the measurement of emissions from standard fires were recommended among a list of high priority needs. Characterization of nuisance signals such as from cooking and automobile exhaust was also high on the list. It was proposed to develop a fire-emulator/detector-evaluator (FE/DE) as a universal test bench for all types of detectors that would simulate the signatures of a wide variety of early fires, as well as common nuisance sources. The current paper describes the measurements made in smoldering fire situations, and how these data might be simulated in a fire emulator for evaluating multi-sensor systems.

CEN 54<sup>2</sup> specifies six different test fires for automatic detection systems. The fires are placed in a room which is about 10 m by 7 m by 4 m high, and the detector under evaluation is located on a flat ceiling 3 m from the fuel centerline. Two of the test fires, TF 2 and TF 3, involve smoldering materials. An electric heater is used to char wood in TF 2. Power is supplied continuously up to the point of flaming, which typically occurs more than 10 minutes into the test. A self-sustained

---

\*This paper is a contribution of the National Institute of Standards and Technology and is not subject to copyright.

Intl. Interflam '96 Conf., 7th Proc. March 26-28, 1996,  
Cambridge, England. Franks, C.A., Grayson, S., Eds.  
Interscience Communications Ltd., London, England, 1996.

smoldering cotton wick is used in TF 3.

Measurements of some of the products of combustion from these two fires have been reported in the literature.<sup>4,5</sup> The data presented here differ in several aspects. For one, the data were measured in the plume close to the fuel source in this study, as opposed to near the ceiling in the previous work. Second, a greater number of chemical species and other physical parameters were measured, and the experiments were repeated enough times to generate meaningful statistics. Third, the laboratory in the current study is smaller than the standard CEN 54 room. The reasons for this and the impact on the conclusions are addressed. Finally, the primary objective of the current work is to quantify the source of important chemical species and particulate matter, the plume momentum, and the thermal energy provided by the fire. This information can be used to specify the source terms of hydrodynamic models of the actual space to be protected, providing guidance to the designer and user of automatic fire detection systems beyond the geometric limitations of the CEN 54 test room.

## FACILITY

The measurements were conducted in a laboratory 3.1 m by 3.1 m by 3.5 m high. A plenum chamber about 1 m deep was located in the upper portion of the room, as shown in Fig. 1. A 1.0 m diameter hole was centered above the test fire in the porous metal sheet that separated the plenum from the lower portion of the room. An exhaust fan drew products of combustion from the plenum at a rate of about 0.4 m<sup>3</sup>/s. Make-up air was supplied into the plenum to maintain a slightly negative pressure in the laboratory. The outlet flow was monitored with a bi-directional pitot probe and strain-gauge-type pressure transducers.

American beechwood was the fuel used for TF 2. It was cut into 10 mm by 20 mm by 35 mm blocks and placed into a conditioning room maintained at 28 °C and 50 % relative humidity. The density of the wood as tested was 760 kg/m<sup>3</sup>. The moisture content was estimated to be 7 % based upon the change in weight between the room-conditioned blocks and oven-dried samples. Twenty-four blocks totaling 124 g ± 3 g were placed upon a grooved, 0.22 m diameter electrical hot plate initially at room temperature (22 °C ± 1 °C). The electrical power to the plate was measured continuously with a Watt meter. Cotton wicks, 4 mm in diameter, were cut into 0.80 m lengths for TF 3. Eighty-seven individual wicks were fastened to a 100 mm ring supported on a metal stand. The total mass of the wick material was 388 g ± 2 g per test. The wicks were ignited at the bottom with a propane torch and the flames were immediately extinguished to produce steady glowing combustion. Mass loss from both TF 2 and TF 3 was continuously monitored by mounting the respective fuel packages on a 1 kg live-load capacity cell with ± 0.2 g resolution. The enthalpies of combustion of wood and cotton as reported from oxygen bomb calorimetry are 20.7 MJ/kg and 16.7 MJ/kg, respectively. The actual heat released during the smolder process was not measured in the experiments, but is likely to be significantly below these levels. Based upon the average fuel consumption rate, the heat release rate for the beechwood was, at most, 2.3 Kw (not counting the electrical power supplied to the hot plate); and for the cotton it was at most 3.2 Kw.

The temperatures in the fire plume were measured with 0.13 mm bare-wire chromel/alumel thermocouples located at various radial and axial positions. The surface temperature of the electrical hot plate was also monitored with a thermocouple. The millivolt signals were compensated with an electronic ice-point and acquired with a data logger at 5 Hz. The axial component of velocity in the plume was measured with a small pitot probe and differential pressure transducers. These data were also collected at 5 Hz.

A 2.0 mm inner diameter, 10 mm outer diameter, jacketed stainless steel probe was built to extract samples from the fire plume. The samples were cooled (or heated) with hot water to quench chemical reactions while avoiding water condensation. The major components of the sample train are shown in Fig. 2. A particle filter and ice-cooled water trap were placed in the teflon/stainless steel sample

line when measuring non-condensable gaseous products. A second particle filter and water adsorbent were located ahead of the oxygen, carbon dioxide, carbon monoxide, and total hydrocarbon process analyzers. The water trap and adsorbent were by-passed and the line was wrapped with heating tape when measuring the water vapor concentration. The response time of the gas concentration measurements was estimated to be between 20 s and 30 s, due to the transit time in the sample line and instrument delay.

An open-path Fourier transform infrared (FTIR) spectrometer was employed across the plume to measure absorption by alkanes, alkenes, alkynes and oxygenated hydrocarbons. The IR spectra were measured at  $2\text{ cm}^{-1}$  resolution and signal-averaged over 64 scans. The evolution of the fires was monitored by collecting a series of 60 spectra over 30 minutes which provided a temporal resolution of 30 s for the time dependent concentration curves. A path-integrated smoke plume extinction coefficient was measured using a photodiode and the 633 nm line of a helium/neon laser.

Additional details on the experimental facility design, the instrumentation and the data acquisition procedure are given in the report by Cleary and Grosshandler.<sup>6</sup>

## RESULTS

A preliminary investigation was made to assess the impact of the room size and exhaust system on the structure of the fire plumes. The requirement for a suitable test space is that the plume not be significantly disturbed from what would be achieved in the full size CEN 54 room. To prevent the build up of heat and combustion products in the test facility, calculations indicated that the hot gases near the ceiling had to be removed. The room exhaust system had a capacity greater than  $1.0\text{ m}^3/\text{s}$ , much more than could be produced by the smoldering fuel. No perturbations to the smoke plume were noticed when the exhaust flow was as low as  $0.2\text{ m}^3/\text{s}$ ; however, this led to smoke filling the test chamber. An exhaust flow of  $0.4\text{ m}^3/\text{s}$  cleared the excess smoke much better, with laser light scattered from smoke away from the fire plume observable only after several minutes into the test. There were not statistically significant differences in mass loss rates or near-field plume temperature measurements as the exhaust flow was varied from 0.2 to  $0.5\text{ m}^3/\text{s}$ . The vertical velocity measured above the fire source prior to ignition (but with the exhaust fan on) remained under  $50\text{ mm/s}$  independent of the size of the exhaust flow. All of the data reported were taken with the exhaust set at  $0.4\text{ m}^3/\text{s}$ . Make-up air was provide through a vent in the wall of the plenum to automatically maintain the room pressure about 28 Pa below the ambient.

### Smoldering/Pyrolyzing Wood (TF 2)

The wood blocks were placed uniformly around two concentric circles on top of the 0.22 m diameter electrical hot plate such that the long dimension of the blocks was aligned with a radius, and the outer edge of the blocks was flush with the outer circumference of the hot plate. The test began by initially applying 1.9 kW of power to the hot plate, which decreased to 1.6 kW as the electrical resistance increased with temperature. The temperature on the surface of the hot plate reached  $600\text{ }^\circ\text{C}$  in  $490\text{ s} \pm 15\text{ s}$  for the five different runs, which was well within the time limit specified in CEN 54<sup>2</sup>.

Mass loss became perceptible about 20 s into the test. The peak pyrolysis rate was  $0.26\text{ g/s} \pm 0.01\text{ g/s}$ , occurring  $620\text{ s} \pm 10\text{ s}$  after heating began. Figure 3 is a plot of the mass loss rate for each test. The repeatability for the first 720 s is remarkable considering that the loss rate is computed from the gradient of the instantaneous mass of fuel measured by the load cell. The wood eventually burst into flames (creating the spikes in Fig. 3), but always after at least 70% of the mass had been lost.

The plume temperatures, averaged over multiple runs,  $0.88\text{ m}$  ( $Z/R=8$ ) above the hot plate are plotted in Fig. 4. The centerline temperature reaches  $45\text{ }^\circ\text{C}$  in 660 s, and decreases with increasing radius in all directions. Velocities at the same axial position are plotted in Fig. 5. The peak vertical component

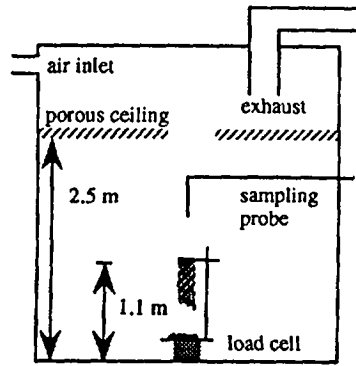


Figure 1. Laboratory arrangement for smoldering cotton fire test.

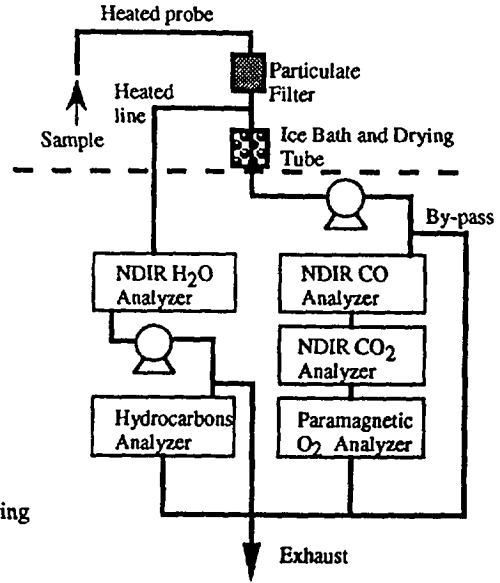


Figure 2. Schematic of gas sampling system.

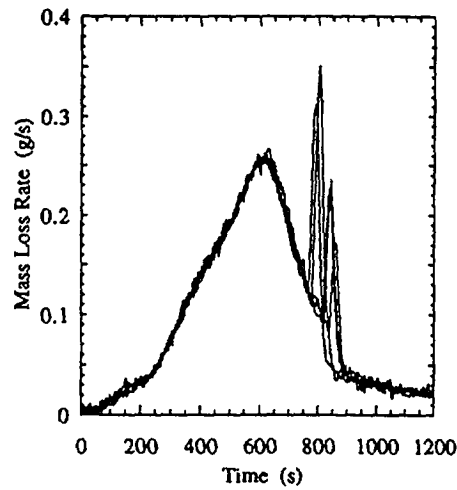


Figure 3. Rate of mass loss in smoldering/pyrolyzing wood tests.

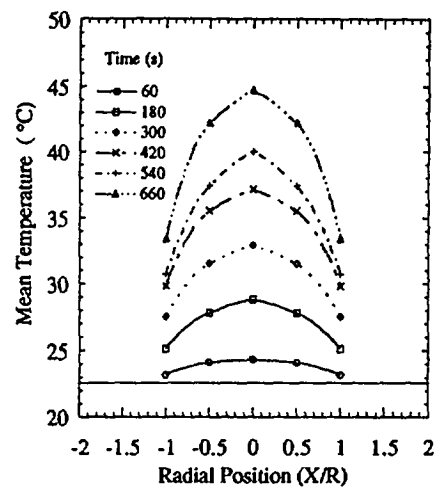


Figure 4. Temperature profiles measured 8R (0.88 m) above the hot plate.

of velocity is slightly over 1.0 m/s on the centerline. Corlett<sup>7</sup> suggests the following correlation between velocity and temperature for steady buoyant plumes:

$$v = (gL \frac{T_0 - T_\infty}{T_\infty})^{1/2} \quad (1)$$

where  $g$  is the acceleration due to gravity,  $L$  is the diameter of the plume,  $T_0$  is the centerline temperature and  $T_\infty$  is the environmental temperature. The value for  $L$  necessary to yield a 1.0 m/s velocity (corresponding to a 45 °C centerline temperature) is 1.3 m, which appears to be a little high considering the velocity profile shown in Fig. 5.

The averages over three runs of the volume fractions of CO<sub>2</sub>, CO and H<sub>2</sub>O measured on the hot plate centerline at an axial position of  $Z/R=8$  are shown in Fig. 6. The CO and CO<sub>2</sub> volume fractions have been decreased to correct for the condensed water, and the background levels of CO<sub>2</sub> and H<sub>2</sub>O have been subtracted so that Fig. 6 represents the true contributions generated by the wood pyrolysis. The ratio of CO to CO<sub>2</sub> is approximately constant at 1/3 throughout the heating period. The water is released from the wood much sooner, but reaches its maximum volume fraction (0.45 %) at about the same point in time. The standard deviation on the H<sub>2</sub>O is much higher than that for either CO or CO<sub>2</sub>.

The volume fractions of hydrocarbon species generated in the smoldering/pyrolyzing wood fire as a function of time are displayed in Fig. 7. The axial position is  $Z/R=8$ . The upper curve represents the total hydrocarbon levels (as methane) measured with the flame ionization detector, and is an average over three runs. The methane (CH<sub>4</sub>), acetaldehyde (CH<sub>3</sub>COH), and acetic acid (CH<sub>3</sub>COOH) are spatial averages across the plume as determined from the FTIR. Quantitative estimates were obtained from the infrared spectra using the following equation:

$$\frac{P_p}{P_c} = \frac{A_p l_c}{A_c l_p} \quad (2)$$

where  $p$  is the partial pressure,  $A = \int A(\nu) d\nu$  is the integrated absorbance over a characteristic band of the target gas, and  $l$  is the corresponding pathlength (taken to be  $2R$ ). The subscripts are used to distinguish between the measurements made in the plume ( $p$ ) above the fire and in the calibration cell ( $c$ ). Carbon monoxide volume fractions are also shown in Fig. 7, and can be seen to agree with the centerline values plotted in Fig. 6.

The laser extinction through the plume  $Z/R=8$  above the hot plate is plotted in Fig. 8.  $I_0$  is the initial unattenuated intensity. The results from two tests show good repeatability. Assuming Beer's law holds, the extinction coefficient can be estimated from  $[\ln(I_0/I)]/l$ . Ten minutes into the test, the extinction coefficient at 633 nm averaged across the diameter (0.22 m) is about  $10 \text{ m}^{-1}$ .

### Smoldering Cotton (TF 3)

Six independent experiments were run using the smoldering cotton fires. Figure 9 shows the cumulative mass loss, normalized by the initial mass of fuel, for the different runs. Four of the mass loss curves (tests 2, 3, 4 and 6) group together, with more than 60 % of the original mass consumed within 1500 s. Run 5 required about 2000 s to be 60 % consumed and run 1 did not exceed this limit during the 3600 s duration of the test. The large variation in burning rates was attributable to the state of the wick material. A higher burning rate occurred if the wicks remained straight and in close contact with each other. If the individual wicks separated from one another and curled outward, more heat was lost to the environment and the chimney-like structure of the initial wick sample was destroyed, affecting the entrainment of oxygen into the smoldering zone. It is unclear which initial conditions lead to the outward curling of the wicks. Figure 10 is a plot of the instantaneous mass loss rate averaged over runs 2, 3, 4, and 6. The mass loss increases at a steady rate for the first 200 s and

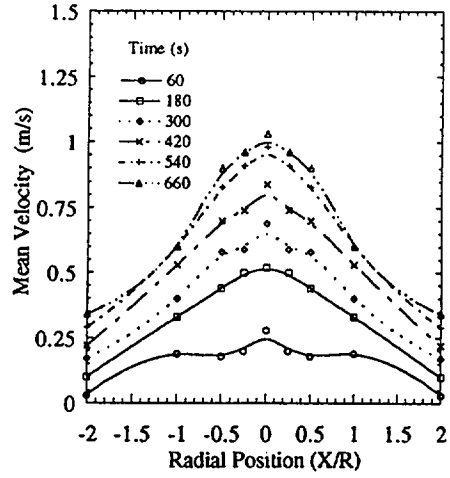


Figure 5. Velocity profiles measured 8R (0.88 m) above the hot plate.

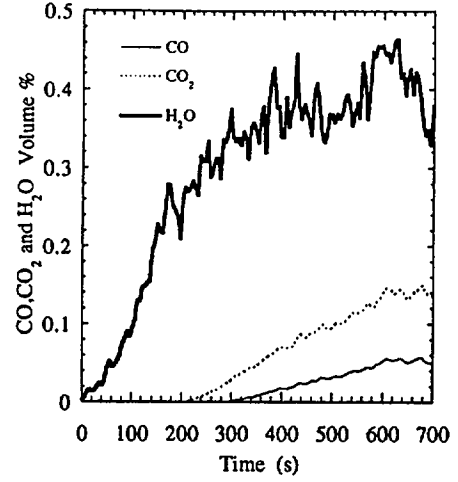


Figure 6. Volume fractions of  $\text{CO}_2$ ,  $\text{CO}$  and  $\text{H}_2\text{O}$  measured on the centerline of the smoldering/pyrolyzing wood fire,  $Z/R=8$ . The average of 3 tests are shown.

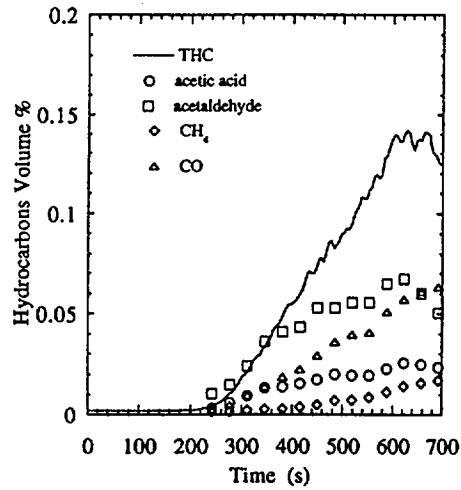


Figure 7. Hydrocarbon volume fractions measured at  $Z/R=8$  above smoldering/pyrolyzing wood fire. The THC is averaged over three runs; other species are averaged over the plume diameter for a single run.

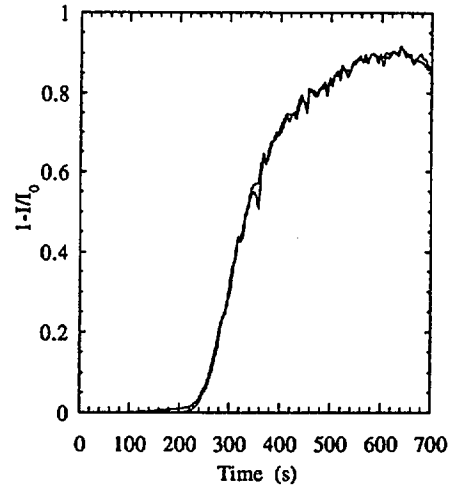


Figure 8. Attenuation of laser light through plume at  $Z/R=8$  above smoldering/pyrolyzing wood.

reaches a plateau of about 0.2 g/s around 500 s into the tests. The range of mass loss rates is about  $\pm 40\%$  of the average value.

The radial variations in temperature were examined 0.05 m ( $Z/R = 1$ ) above the top of the wick. The centermost temperatures were within 20 °C of the those measured half way to the edge of the fuel source ( $R/2$ ). Temperatures at the edge of the source ( $R$ ) rarely exceeded 40 °C, and were as much as 100 °C below the centerline values. This suggests a top-hat profile near the fuel surface with a high temperature uniform core increasing in time to about 120 °C and a close-to-ambient value at the edge of the fuel. Figure 11 shows the temperatures measured with time on the fuel centerline 0.16 m ( $Z/R = 3.2$ ) above the top of the wicks. The solid line represents the average at each time of runs 2 and 3. The average temperature increases steadily for 650 s to about 70 °C, and thereafter increases at a slower rate to a maximum of 88 °C at 1500 s. Temperature excursions exceeding 100 °C can be seen in the run-to-run deviations plotted as symbols in the figure.

Figure 12 is a plot of the vertical component of velocity on the centerline 0.16 m above the top of the fuel surface. The solid line represents the average of runs 2 and 3; the symbols are representative of the run-to-run variations. The velocity plateaus near 650 s into the test at a value just over 1.0 m/s.

The major product gases measured in the smoldering cotton fire were  $\text{CO}_2$ ,  $\text{H}_2\text{O}$  and  $\text{CO}$ . The concentrations are shown as a function of time in Fig. 13. Each curve represents the average of runs 2, 3 and 4. The  $\text{CO}_2$  and  $\text{CO}$  were corrected for the removal of water vapor. The background levels of  $\text{H}_2\text{O}$  and  $\text{CO}_2$  have also been subtracted. The concentrations of carbon oxides build up in a similar manner, with a 1:3 ratio for  $\text{CO}/\text{CO}_2$  holding remarkably well for the entire test. The water is released earlier; after about 600 s the  $\text{H}_2\text{O}/\text{CO}_2$  ratio is close to unity.

The laser intensity through the plume 0.01 m above the smoldering cotton wicks is plotted in Fig. 14, normalized by the initial unattenuated intensity. The solid line is the average of tests 2, 3, 4, and 6. The extinction coefficient at 633 nm (from Beer's law), 600 s into the test, is  $16 \text{ m}^{-1} \pm 6 \text{ m}^{-1}$  assuming an extinction pathlength equal to the fuel cylinder diameter.

## DISCUSSION AND CONCLUSIONS

Pfister<sup>4</sup> and Jackson and Robins<sup>5</sup> measured the ceiling temperatures and combustion products in the TF 2 and TF 3 fires burning in a standard CEN 54 room. Their reported temperature increases and volume fractions of  $\text{CO}$  and  $\text{CO}_2$  are 6 to 8 times lower than those measured here in the smoldering wood fire, 0.88 m above the hot plate. The hydrocarbon levels measured in a previous study<sup>4</sup> are a factor of 60 times lower than those measured here, an inconsistency suggesting a possible sampling problem in the older study or a difference in operating procedure. Comparing the previous measurements taken near the ceiling in TF 3, the values of  $\text{CO}_2$ ,  $\text{CO}$  and temperature increase measured 0.16 m above the cotton wick in the current study are greater by over an order of magnitude. Modeling of plume entrainment and the ceiling jet are required to ascertain if the different studies are in general agreement with each other.

Preliminary time signatures suggested for these two smoldering/pyrolyzing fires are plotted in Figs. 15 and 16. Note that they refer to predicted centerline values 0.88 m and 0.16 m above the TF 2 and TF 3 fires, respectively. The equations for these curves and their justification are given elsewhere<sup>6</sup>. As more testing is completed, additional species volume fractions (e.g.,  $\text{H}_2$ ,  $\text{CH}_4$ ,  $\text{NO}$ ) and electromagnetic spectra will be added to these signatures. The standard deviation and characteristic fluctuating frequencies will also be accumulated. With this information, computational fluid dynamics can be used to model the transport of heat and species throughout the CEN 54 test room or any other volume in need of protection. This modeling approach has been used in a number of situations<sup>9, 10, 11</sup> to determine the impact of room geometry, distance from the fire, and room ventilation on the likely response of a fire detector. The response of a multi-criteria detector to a smoldering fire can also be

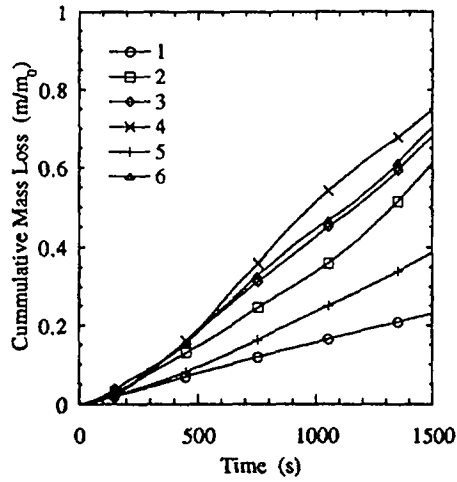


Figure 9. Mass loss normalized by initial mass of smoldering cotton wicks.

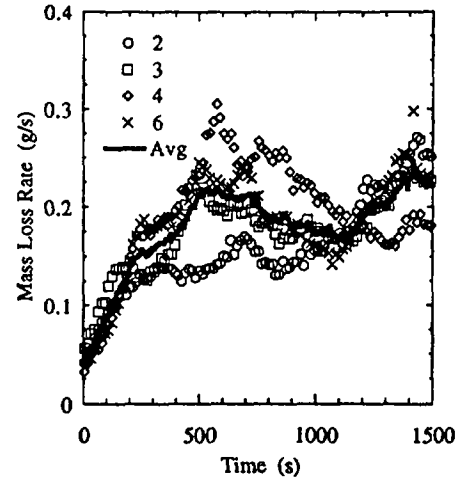


Figure 10. Rate of mass loss in smoldering cotton fire. Solid line is average of four faster burning tests.

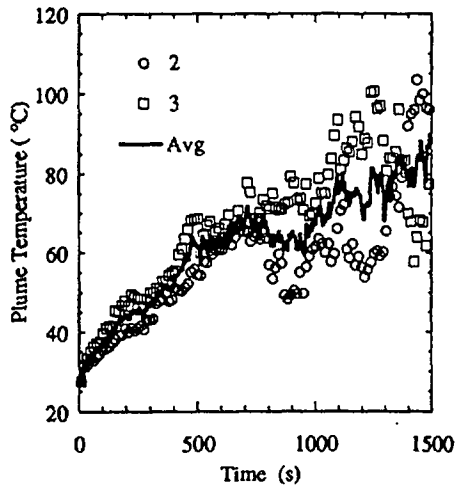


Figure 11. Centerline temperatures measured 0.16 m above the smoldering cotton wicks. Solid line is the average of runs 2, 3, and 4.

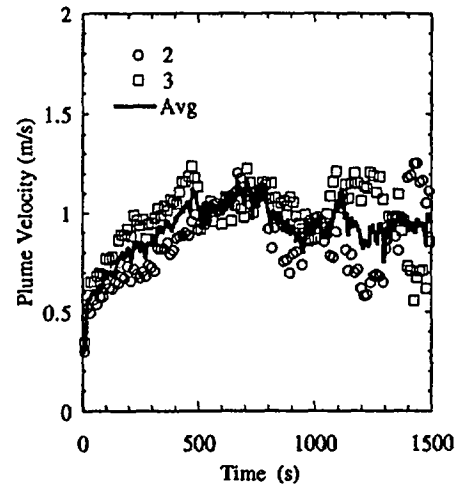


Figure 12. Vertical velocity measured 0.16 m above the top of the smoldering cotton wicks. Solid line is the average of runs 2, 3, 4, and 6.



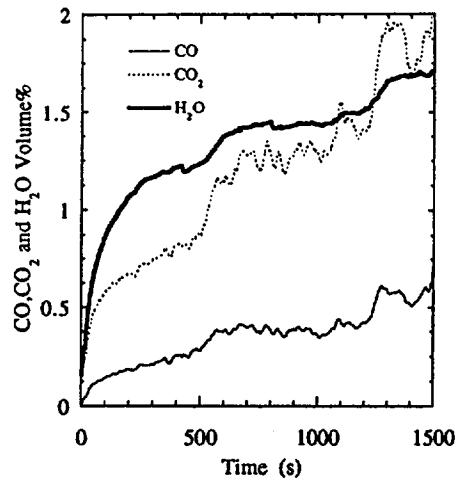


Figure 13. Concentrations of CO<sub>2</sub>, H<sub>2</sub>O and CO measured in smoldering cotton fires. CO<sub>2</sub> and CO are averages of tests 2, 3, and 4; H<sub>2</sub>O is average of tests 2 and 4.

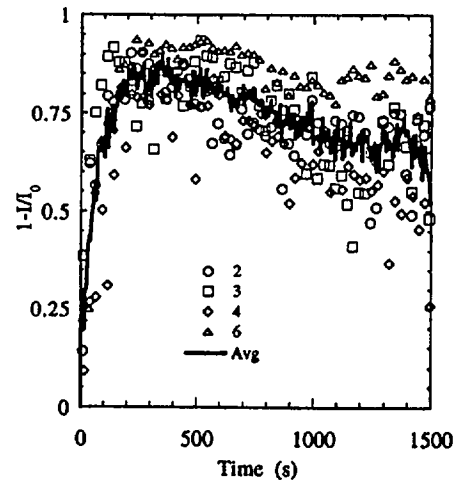


Figure 14. Attenuation of laser light through plume 0.01 m above top surface of smoldering cotton wicks. Solid line is average of tests 2, 3, 4, and 6.

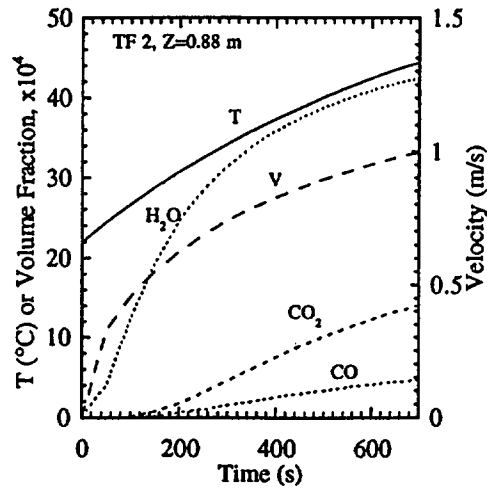


Figure 15. Suggested partial signature for smoldering/pyrolyzing wood fires (TF 2) used to evaluate multi-criteria detection systems.

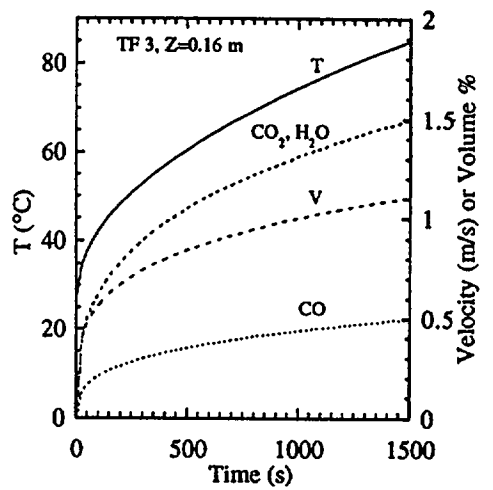


Figure 16. Suggested partial signatures for smoldering cotton fires (TF 3) used to evaluate multi-criteria detection systems.

evaluated by exposing the sensors to the temperatures and concentrations predicted by the fluid mechanical models. The original concept for a fire-emulator/detector-evaluator was introduced<sup>3,8</sup> expressly for this purpose. The FE/DE would minimize test-to-test variations, permit evaluation (under identical conditions) single element gas, smoke, and thermal sensors, as well as multi-criteria detectors; accommodate line-type detectors, new combinations of existing sensors, and novel devices operating on new principles; and minimize the emission of noxious combustion gases and the precautions necessary for live-fire tests. The attributes desired in a universal FE/DE are described in Cleary and Grosshandler<sup>6</sup>, along with the range of operational variables envisioned. The data summarized in Figs. 15 and 16 are, thus, key to the successful implementation of the FE/DE concept.

## ACKNOWLEDGEMENT

The authors wish to acknowledge the assistance of Michelle King in taking the initial data and William Mell for his numerical calculations of the flow field.

## REFERENCE LIST

1. *UL 217: Standard for Single and Multiple Station Smoke Detectors*, Underwriters Laboratories, Inc., Northbrook IL, 1993.
2. *EN 54: Components of Automatic Fire Detection Systems; Part 9. Fire sensitivity test*, European Committee for Standardization, July 1982.
3. Grosshandler, W.L. (editor), *Proceedings of the 1995 Workshop on Fire Detector Research*, NISTIR 5700, August, 1995.
4. Pfister, G., "Detection of Smoke Gases by Solid State Sensors - A Focus on Research Activities," *Fire Safety Journal* 6, 165-174 (1983).
5. Jackson, M.A., and Robins, I., "Gas Sensing for Fire Detection: Measurements of CO, CO<sub>2</sub>, H<sub>2</sub>, O<sub>2</sub>, and Smoke Density in European Standard Fire Tests," *Fire Safety Journal* 22, 181-205 (1994).
6. Cleary, T., and Grosshandler, W., *Signatures of Smoldering Fires for Use in a Fire-emulator/ Detector-evaluator*, NISTIR, National Institute of Standards and Technology, in press, 1996.
7. Corlett, R.C., "Velocity Distributions in Fire," *Heat Transfer in Fires: Thermophysics, Social Aspects, Economic Impacts*, Blackshear, D.L., ed., pp. 239-254, 1974.
8. Grosshandler, W.L., "Towards the Development of a Universal Fire Emulator/Detector Evaluator," *Proceedings, Automatische Brandentdeckung, AUBE '95*, Duisburg, Germany, p. 363, April, 1995.
9. Baum, H.R., McGrattan, K.B., and Rehm, R.E., "Mathematical Modeling and Computer Simulation of Fire Phenomena," *Fire Safety Science - Proceedings of Fourth International Symposium*, T. Kashiwagi, ed., IAFSS, USA, pp. 185, 1994.
10. Forney, G.P., Bukowski, R.W., and Davis, W.D., *International Fire Detection Research Project - Field Modeling: Effects of Flat Beamed Ceilings on Detector and Sprinkler Response*, Technical Report Year 1, National Fire Protection Research Foundation, Quincy, MA, October 1993.
11. Satoh, K., "Study of Early and Reliable Fire Detection in Air-conditioned Rooms," *Fire Safety Science-Proceedings of the Fourth Int'l Symposium*, T. Kashiwagi, ed., IAFSS, USA, p. 173, 1994.